

MECHATRONIC SERVO SYSTEM APPLIED TO A SIMULATED-BASED AUTOTHROTTLE MODULE

Rafael Coronel Bueno Sampaio, rafaalc@sc.usp.br

Mechatronics Lab-SEM-EESC-USP, São Carlos, Brazil

Marcelo Becker, becker@sc.usp.br

Mechatronics Lab-SEM-EESC-USP, São Carlos, Brazil

Abstract. *Flight Simulation represents a very important support tool on avionic systems conception, through which one can emulate atmospheric phenomena as well as the aircraft itself. It also makes possible to experiment both flight mechanical and dynamical behaviors with a high level of reliability. In practical terms, that contributes considerably to reduce project costs, once it allows the simulation, in ground, of many real scale aircraft flight circumstances/situations. In this work we propose the construction of a mechatronic autothrottle system, which is part of a simulated-based AFCS (Automatic Flight Control System) project composed by a digital PID controller and an embedded microcontrolled physical throttle quadrant. The designed autothrottle system is a full autonomous device which promotes the aircraft IAS (Indicated Air Speed) adjustment by means of the aircraft inertial acceleration management (calculated in three aircraft axis). Initially we described all methods applied on the throttle quadrant design. We emphasized the DC motor full characterization and an analogical PID controller modeling process, both using experimental techniques on the construction of a servo system. As the digital PID controller calculates the right amount of power delivered to the simulated aircraft engines, it can be seen that the physical throttle levers also get their angular positions to the corresponding value, according to the aircraft engine power levels demanded at that time. In real autothrottle systems, on-line throttle quadrant angular reposition is a safety requirement to avoid catastrophic hazards/events due to overloading of engine structural limits, preventing crew to demand erroneous levels of power. Experimental techniques were used on obtaining the DC motor full transfer function by acquiring both electrical and mechanical most important motor parameters. These methods took into account some simplification hypotheses because the motor used in this work was a low scale device. The three PID parameters (proportional, derivative and integrative gains, respectively) were determined through a detailed investigation of the analogical PID controller circuitry. Furthermore, the analogical PID controller transfer function was determined based on the related parameters. A complete MATLAB/SIMULINK model was developed for the mechatronic servo system so that a complete analytical evaluation was established. Previous simulation analysis in SIMULINK had shown very encouraging results for both DC motor and analogical PID controller transfer functions obtained through the use of experimental techniques and the predefined simplification assumptions. Excellent results were also achieved in practice. The mechatronic servo system designed responded very well to new reference entries for the lever angular position adjustment in real time, as the controller demanded on-line new aircraft engine power.*

Keywords: AFCS, autothrottle system, DC motor characterization, digital controller, servo system.

1. INTRODUCTION

The correct computational application of the mathematical aircraft models results in outstanding flight simulators for a huge number of applications related to aerospace industry projects. Ground-based flight simulators provide pilots with the "feel" of flight by using a combination of simulator motions and visual images. The more sophisticated flight simulators provide six degrees of freedom to the simulator cockpit, driven by computers, to produce the desired motion based on the so-called aircraft equations of motion (Rolfe, 1983). Those ground-based flight trainers perfectly reproduce the aircraft cockpit, allowing crew to interact with the embedded avionic systems, just as they were handling real avionic systems. This study is part of a previous work which aims the construction of low-cost full simulated-based AFCS (Automatic Flight Control System) and physical avionic systems for the Embraer EMB-170. These avionic systems can be attached to the computer which generates the dynamics of such aircraft, so that it is possible to offer MMI (Man Machine Interfaces), similar to the real aircraft ones (Sampaio, 2008). In that work, *Microsoft Flight Simulator 2004* was used to generate almost 1400 aircraft flight parameters such as the aircraft state vector of flight derivatives necessary on solving the equations of motion. A software interface named SGVV (Portuguese acronym for Flight Parameters Management System) was specially written to read and write *MSFS 2004* offset memory addresses which contains current values of flight variables. The ability of reading and writing on the simulation is what allows closed loop control systems to be designed, thus allowing the construction of low cost real-time avionics systems as well.

In the present work we propose the design of a mechatronic autothrottle system, composed by a throttle quadrant which, likewise in real aircrafts, provides pilot with the visual precise and current level of power delivered to the aircraft's engines for a specific flight condition. A full digital autothrottle system was implemented for the aircraft's IAS (Indi-

cated Air Speed) adjustment by means of the aircraft inertial acceleration management. The digital autothrottle system was embedded into the AFCS module in SGVV. Heuristic methods were used to the implementation of the digital PID recurrence equations and they based on *Tustin* approximation and backward difference approximation. *Ziegler-Nichols'* methods were employed for the estimation of the digital PID parameters, once the determination of the aircraft transfer function is not the scope of this project nor the propulsion system modeling. Thus, it was possible to model the digital PID controller through some experimental methods, based exclusively on observation of the aircraft dynamical behavior for each phases of flight (Ogata, 2000).

The fine adjustment techniques proposed here consist of one of the most important components of the digital PID controller enhancement and has been intensively studied, following the work of (Oliveira, 2005). Some modifications in the three PID recurrence equations are proposed for the robust controller to be achieved and the flight envelopes as well.

For the physical throttle quadrant design, still in (Oliveira, 2005), experimental practical methods were used on the full characterization of two low scale DC motors, coupled to reduction gearboxes and a sense potentiometer each one. Additionally, for the complete achievement of a servo-mechanic system, an analog PID controller was successfully designed through the modeling of an electronic schematic using operational amplifiers. A *Microchip* microcontroller was used as a "bridge" between the throttle quadrant and the flight simulator, managing the full duplex communication to SGVV (via RS-232 PC port) and handling all control signs to the online adjustment of the levers angular repositioning process, as SGVV sends angular repositioning commands.

In the background, an exhaustive complete study of longitudinal flight dynamics was developed (Pratt, 2005), (Etkin and Reid, 1996). For the understanding of the aircraft equations of motion we followed the work of (Roskan, 2001). A SIMULINK aerospace toolbox was used, so that a reliable control system could be analyzes and achieved (Rauw, 2001).

2. THE AUTOTHROTTLE SYSTEM PROBLEM FORMULATION

Spacecraft's IAS adjustment involves, in practice, the control of the vehicle velocity vector, composed by speed and the flight-path angle γ , both related to the longitudinal control. Former is provided by thrust control, and the latter by lift control via elevator deflection or wing flaps. Obviously, the main initial response to opening the throttle (increasing the thrust) is a forward acceleration. The main initial response to elevator deflection is a rotation in pitch, with subsequent change in angle of attack and lift, and hence a rate of change of flight-path direction. However, it is known from the aircraft longitudinal equations that there is a clearly defined relation between the speed and the pitch control. The ultimate result of moving the throttle at fixed elevator angle (when the thrust line passes through the CG) is a change in γ without change in speed. But the initial response to throttle is a change in speed (Etkin and Reid, 1996).

In this work we considered an alternative concept that does not require any knowledge of the final correct pitch attitude, but that uses speed error alone. Although the control module related to this project also comprehends the pitch control δ_e to suppress the phugoid, which is a very long period oscillation, our goal here is to achieve an efficient and robust speed controller concerning exclusively to speed itself. The command vector c is composed simple by the reference speed u_c , and the feedback signal is the actual speed u . For output we choose simple the speed, that is, $y = [u]^T$. The control vector also acts only over thrust $c = [\delta_p]^T$, where δ_p is the propulsion control action. Figure 1 shows the closed loop block diagram for the IAS speed controller.

Basically, the throttle quadrant must allow crew to establish an interface with the aircraft propulsion system. When the EMB-170 propulsion system autothrottle system is disengaged, the pilot can (theoretically) input a power level from 0 to 100% of the available engine power. Obviously, mechanical and structural limits are established so that the the correct application of power must be supervised. Generally, the FADEC (Full Authority Digital Engine Control) is the avionic system which manages the engine functions through a thrust management system. In this project, the autothrottle module is also in charge of managing N1 and N2 engine speed limits, trimming their levels appropriately. The autothrottle system architecture is shown in Fig. 2.

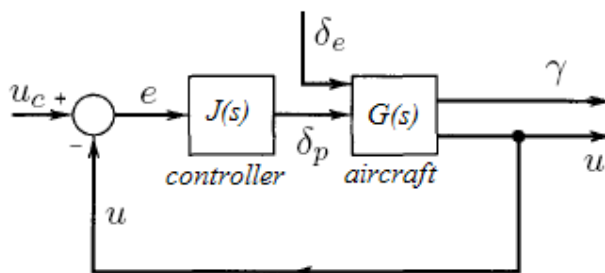


Figure 1. Aircraft speed controller block diagram. In this project it was only considered the direct influence of speed u error on the calculus of thrust control signals δ_p .

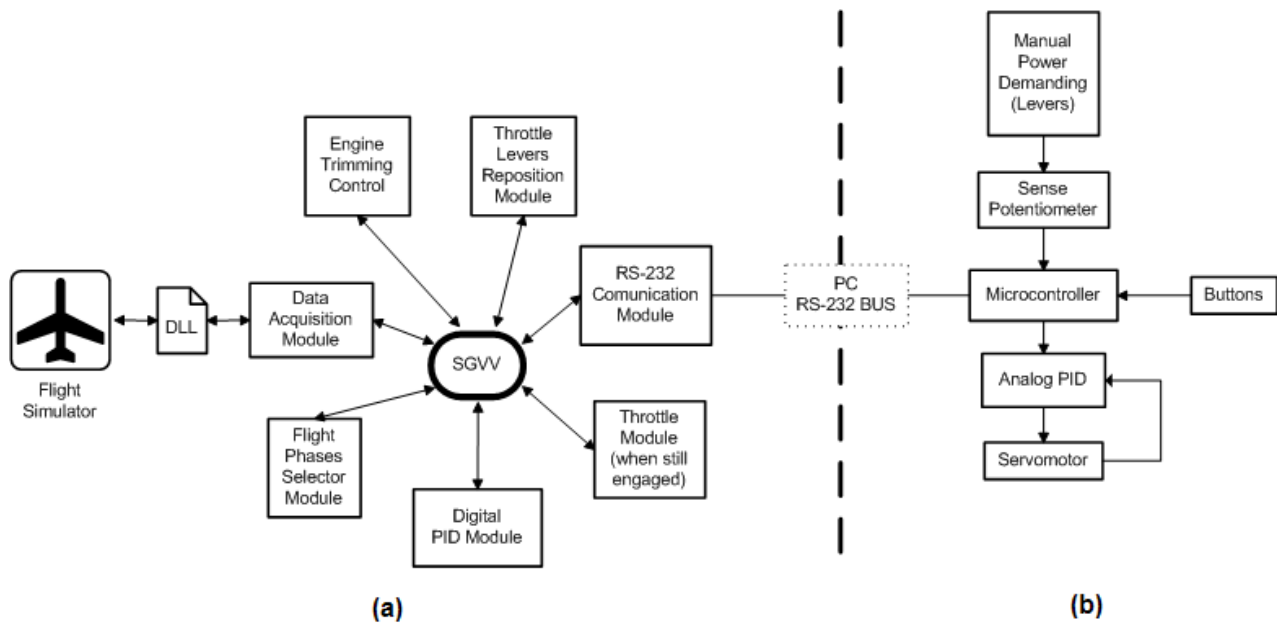


Figure 2. Architecture of the autothrottle system designed for this work. The physical throttle quadrant is a full-duplex RS-232 communication device (b) which sends/receives control signs to/from the flight simulator through SGVV interface (a). SGVV is composed by different modules and accesses the flight simulator memory offset *via* a dedicated DLL file.

3. INERTIAL ACCELERATION MANAGEMENT PROBLEM FORMULATION ON IAS ADJUSTMENT

The IAS control problem is defined as the determination of the right amount of power provided to the aircraft engine that generates a given set of desired accelerations specified by a flight control law which transfers algorithms' commands (which are merged into the digital PID module) given by a defined acceleration envelope. As this work is related to the construction of a brand new AFCS, it is reasonable to assume that determining the referred above aircraft acceleration envelope is also needed, prior to the implementation of PID routines. Some empiric assumptions were necessary in order to get this process started (Pratt, 2005).

3.1 Acceleration Envelope Determination

Flight essays were run with the aircraft flying in cruise steady mode in order to study and then obtain the curve that best represents the aircraft acceleration envelope for that phase of flight. It was considered that the aircraft current acceleration should be given as a direct function of the IAS error, that is, there is a proper value for the aircraft acceleration for each difference between the target speed and the current speed. Furthermore, the aircraft acceleration envelope should respect the human body acceleration limits. In order to simplify the analysis, *a priori*, it was assumed that aircraft acceleration should not exceed 1G, that is, the acceleration envelope should be trimmed at around $9,8m/s^2$ ($32,15ft/s^2$). The aircraft acceleration envelope determined can be seen from Fig. 3. As it was expected, the curve is approximately linear. This stage is very important once the flight envelope determined here will be used as benchmark for the digital PID controller design. By visually inspecting the interpolated curve from Fig. 3, it is possible to obtain the angular coefficient of the function, so that the target acceleration can be given by:

$$accel_{target} \approx 0,049 \cdot delta_{vel} \quad (1)$$

Where $delta_{vel}$ is equivalent to the difference between the target speed and the current speed.

Digital PID controller will take Eq. (1) to calculate the best control action as the reference value to the engine power management. Engine power management is executed by the correction on the the throttle levers position in the simulated aircraft. It means that the virtual levers change its angular position, as the digital PID controller calculates the best power decreasing or increasing rates. Therefore, PID controller manages the aircraft inertial acceleration through an output control signal δ_p , which actually acts over the engine by means of controlling the lever angular position on the virtual throttle quadrant. In practice, controller must provide flight simulator with binary incremental/decremental values in a range from 0 to 1024 (10 bits), which will affect the angular lever position and so both engine's power.

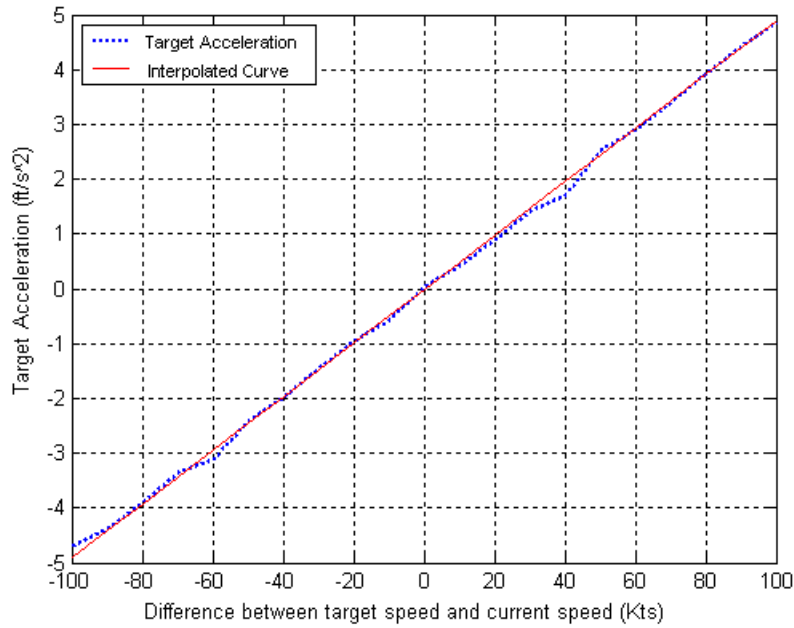


Figure 3. Relationship between target acceleration and the difference between current speed and required speed. Aircraft current acceleration is a direct function of the IAS error. Target acceleration operational envelope is give by a linear function as shown by the continuous line.

3.2 Digital PID Controller Recurrence Equations

The digital PID controller implemented in this work consists on an algorithm based on the recurrence equations proposed in (Oliveira, 2005). These algorithms consider the positional form with backward difference approximation to the integrative term (I) and *Tustin* approximation to derivative term (D), whose control laws can be respectively represented by:

$$P(k) = K_p[\beta r(k) - y(k)]; \quad (2)$$

$$I(k) = I(k - 1) + \frac{K_p T}{T_i} e(k - 1) \quad (3)$$

$$D(k) = \frac{2T_d - TN}{2T_d + TN} D(k - 1) + \frac{2K_p T_d N}{2T_d + TN} (y(k) - y(k - 1)) \quad (4)$$

$P(k)$, $I(k)$ and $D(k)$ correspond, respectively, to proportional, integrative and derivative control signals. K_p is the proportional gain, T_i is the integrative time and T_d is the derivative time. $r(k)$ is the reference signal (which represents the target acceleration), $y(k)$ is the output signal (control signal, which represents the increasing or decreasing rate on lever position) and $e(k)$ is the error. T is the sample rate of data acquisition, N is one important parameter that optimizes derivative action and assures the controller normal operation. For the proportional action, a fine tuning parameter β is also employed (Oliveira, 2005), acting over the output signal.

3.3 Heuristic Methods for Optimization of the Effects of Zeros and Poles to Controller Performance

The determination of K_p , T_i and T_d followed the 2nd *Ziegler-Nichols* method proposed by (Ogata, 2000), since this project does not aim to determine the aircraft exact transfer function (neither the propulsion system mathematical model). Once both K_{cr} and P_{cr} are found, it is possible to determine the values of K_p , T_i and T_d by *Ziegler-Nichols* look-up equations (Ogata, 2000). It turns out necessary to analyze the final PID equation in order to propose some changes on it, as well as the use of some digital filters. The PID equation, following *Ziegler-Nichols* methods, can be written as follows:

$$G_c(s) = 0,075K_{cr}P_{cr} \frac{\left(s + \frac{4}{P_{cr}}\right)^2}{s} \quad (5)$$

In first analysis, it is necessary to pay close attention to Eq. (5). The equation has one pole at the origin and a double zero in $s = -\frac{4}{P_{cr}}$. This contributes to the elimination of the stationary state error. However, it can still be observed from

Eq. (5) that the greater the error becomes, the greater becomes the output signal (control signal). It certainly causes the throttle actuators to be unstable which, by the way, becomes the system also unstable. At best, it takes much longer to stabilize the system, causing undesirable overshoot rates.

The reset-windup effect was prevented by implementing an anti-reset-windup filter, which acts over the integrative band (Oliveira, 2005). The filter works under the following condition:

$$\Delta u_i(k) = 0, \text{ if } |e(k)| \geq e_{max} \quad (6)$$

The term $u_i(k)$ refers to integrative band contribution on PID controller and e_{max} is maximum desired error, which is experimentally determined by observing and proposes the canceling of integrative contribution when it reaches the maximum value for the error, previously set.

As for the derivative action, it also can present values that contribute directly to the system instability in some circumstances. In example, derivative band introduces an uncontrollable gain increase at high frequencies. This is called quick derivative effect. As it can be seen from the right hand of Eq. (5), derivative term presents one pole at the infinite. That proves the above-mentioned instability at high frequencies. Once an undefined increasing in frequency occurs, derivative gain also increases and then makes the system out of control. The filter applied in this case aims to add one pole to the derivative contribution on the general PID action. That results in the following derivative term:

$$D(k) = \frac{K_p T_d s}{1 + \frac{T_d}{N} s} \quad (7)$$

where N is a constant that assures the realizability of the controller when operating at high frequencies. Values of N of $3 \leq N \leq 20$ are usually adopted (Oliveira, 2005).

As proposed in (Oliveira, 2005), is also convenient to introduce a proportional band fine tuning coefficient β , into the proportional action, as it is shown in Eq. (2). Indeed, flight tests showed very good results especially on eliminating the stationary state error. Improving on transitory response was also successfully achieved.

Although it is known that proportional band fine adjustment (by the use of β) itself eventually results in a good performance, an autothrottle system demands a very precise action from the controller. Therefore, as it concerns to an AFCS application, it is strongly recommended that all three enhancement methods are simultaneously employed, in order to achieve an improvement of the final responses.

After this detailed analysis, 2nd *Ziegler-Nichols* method was applied in order to obtain the digital PID parameters. Aircraft responds distinctly for each phases of flight as its dynamics changes for each flight situations. Hence, PID will assume a different set of values to each one. However, cruise steady flight was taken as the benchmark scenario for the PID parameters calculation. Thus, altitude was set constant as the aircraft was requested to hold speed at 250 Kts. Values of T_i and T_d were set to infinite and zero respectively. At a certain point of the flight test the aircraft inertial acceleration was expected to present an oscillatory behavior, as K_{cr} slowly started raising from zero. At a value of $K_{cr} \approx 284$, acceleration presented a maintained oscillatory behavior, and a $P_{cr} \approx 23s$ (signal period) was noted. Applying the values of K_{cr} and P_{cr} to the *Ziegler-Nichols* lookup equations, it was found a proportional gain $K_p \approx 170$, an integrative time $T_i \approx 11$ and a derivative time $T_d \approx 2,87$.

4. THE THROTTLE QUADRANT ASSEMBLY

The throttle quadrant designed for the autothrottle system consists basically on a servo-system, composed by two low scale and low current consumption DC motors, an analog PID controller and linear potentiometers whose signals are feedback. Each aircraft's engine power lever brings also additional linear potentiometers in their respective bottoms, through which both levers were coupled to the DC motor shafts. These potentiometer send throttle signals to the microcontroller and the last one, in turn, sends increase/decrease thrust commands to the flight simulator through SGVV. On the other hand, digital PID controller calculates appropriated aircraft acceleration envelopes and sends (on-line) new entries of the lever angular position to the microcontroller which, by the way, sends equivalent commands to the analog PID controller for both levers' new angular positions. The following sections describe the analog PID controller design, the full characterization of both DC motors and the microcontrolled signal conditioning to the management of the throttle quadrant.

4.1 The Analog PID Controller Design and Parameters Estimation

An analog PID controller was designed to achieve a servomechanism to the throttle quadrant. In order to analyze the control actions, PID controller's transfer functions was found based on the electronic schematics seen in Fig. 4, and is represented by the following equation:

$$G(s) = \frac{R_2 R_6 R_8}{R_1 R_5 R_7} - \frac{R_{10}}{R_9} \cdot \frac{1}{1 + R_{10} C_1 s} - R_{11} C_2 s \quad (8)$$

In practical terms, the three PID controller parameters can be determined by some discrete electronic components relations and combinations. In this case, proportional gain $K_p \approx \frac{R_8}{R_7}$, integrative time $T_i \approx R_9 C_1$ and derivative time $T_d \approx R_{11} C_2$. A SIMULINK model was set up, so that diverse values for the discrete components could be tried out in order to achieve an appropriated response from the controller. Thus, based on this model, the controller responded satisfactorily to values for proportional gain $K_p = 10$, integrative time $T_i = 0.01$ and derivative time $T_d = 0.1$.

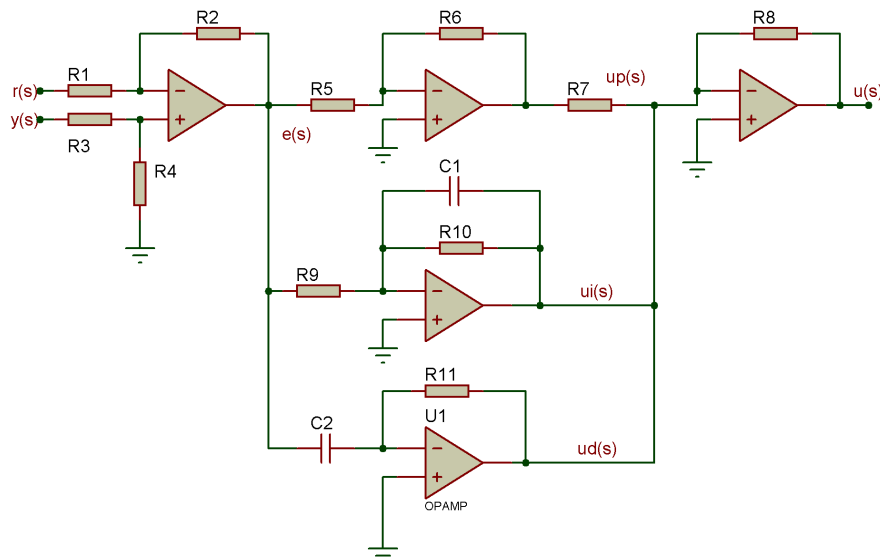


Figure 4. Electronic schematics for the analog PID controller responsible for the motor angular shaft reposition, which is coupled to the throttle levers.

4.2 The DC Motor Full Characterization Process

Both DC motors used in the throttle quadrant are low scale and low current consumption motor drives each one coupled to a reduction gearbox. There is a linear potentiometer also coupled to the motor shaft which works as a voltage sensor for the feedback control system. Thus, it turns the whole assembly to a servo system. DC motor full characterization was based on practical laboratory experiments which allowed us to obtain a very reliable transfer function to describe the motor dynamics, from the determination of both mechanical and electrical related parameters. Following the methods described by (Oliveira, 2005), the DC motor's transfer function can be represented by the following:

$$M(s) = \frac{k_m}{s[T_m s + 1]} \quad (9)$$

where k_m and T_m are defined as the DC motor both gain constant and time constant respectively. These constants are respectively defined by the following equations:

$$k_m = \frac{k_t}{R_a k_b + k_{cem} k_t} \quad (10)$$

$$T_m = \frac{R_a J}{R_a k_b + k_{cem} k_t} \quad (11)$$

where k_b is the EMF (Electromotive Force) constant, R_a is the coil resistance, k_{cem} is the back EMF force, k_t is the torque constant and J is the shaft moment of inertia. The parameter denoted as L_a is the coil inductance and it was neglected since the DC motor is a very small scale device (Oliveira, 2005). All DC motor parameters were determined following the previous referenced methods and are listed in Table 1.

Table 1. DC motor mechanical and electrical parameters obtained experimentally by using practical laboratory methods.

Parameter	Value	Dimension
R_a	14	Ω
k_{cem}	0,0411	-
k_t	0,0411	-
J	$240 \cdot 10^{-9}$	$\frac{Nms^2}{rad}$
k_b	$18,83 \cdot 10^{-6}$	-

Replacing the values of each parameter from Tab. 1 in Equations (10) and (11), the following DC motor transfer function is obtained:

$$M(s) = \frac{21,04}{s[0.0017s + 1]} \quad (12)$$

Another important parameter which must be taken into account is the gearbox reduction transfer function in order to insert it into the closed loop control. As the reduction relation is of about 100:6, the gearbox transfer function can be given as a gain, represented by an attenuation which can be given by n , as follows:

$$n \approx 60 \cdot 10^{-3} \quad (13)$$

The feedback linear potentiometer must be also included as part of the final plant. In *Laplace* domain, the linear potentiometer transfer function can be expressed by:

$$P(s) = \frac{\alpha}{s^2} \quad (14)$$

where α is the angular coefficient of the potentiometer output voltage curve *versus* time.

Since all servo system components were modeled, it is now possible to obtain a full closed loop schematics, in order to analyze its responses to input signals. Figure 5 shows the servo system schematics including analog PID controller, DC motor, reduction gearbox and linear feedback potentiometer transfer functions.

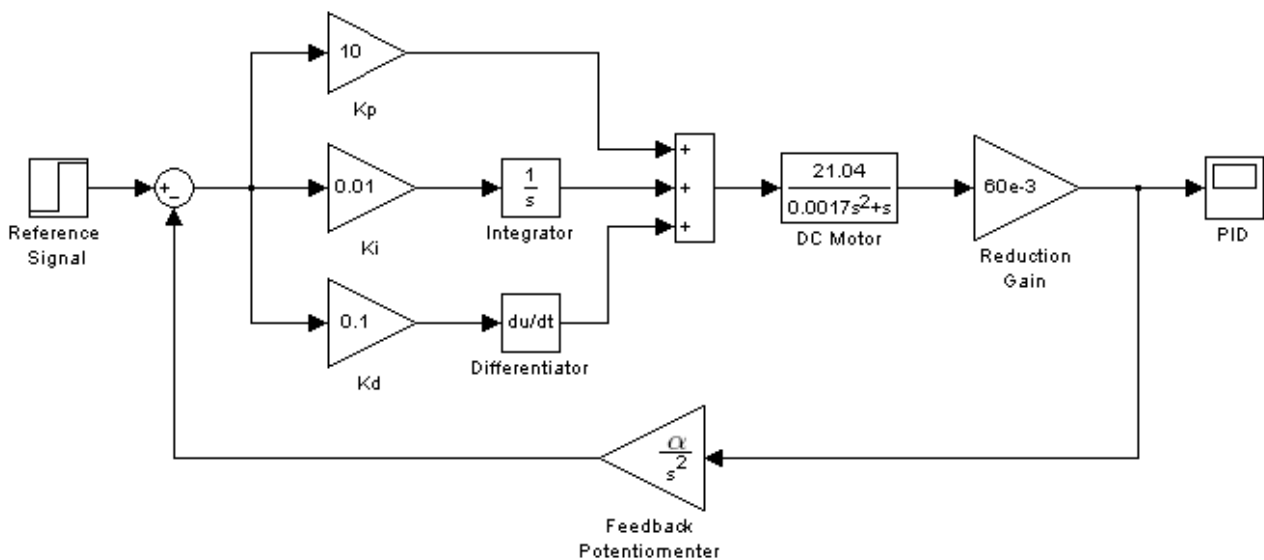


Figure 5. Schematics of the complete servo-system designed to the throttle quadrant levers angular repositioning process.

4.3 Microcontrolled DC Motor Angular Position Management

DC motor shaft angular position control primarily depends on a reference signal incoming from SGVV digital control module. However, the module only calculates the right position of the throttle levers based on the current amount of power requested to the aircraft engines. It turns out important to send this position to the physical lever, which is achieved by the PC RS-232 communication port, where SGVV writes the RS-232 bus with proper commands addressed to the

microcontroller. The last one, by the way, must provide analog PID controller with proper reference signals to the correct shaft angular adjustment. PWM (Pulse Width Modulation) was used to vary the reference tension values to the PID controller, since it is more convenient to the microcontroller to work with digital signal processing. The following transfer function was obtained to the precise calculation of the reference signal to the angular shaft positioning process:

$$P_s \approx 10,38 \cdot 10^{-3} \cdot P_{m.s} + 650 \quad (15)$$

where P_s is the PWM duty cycle value and $P_{m.s}$ is the lever position calculated by SGVV digital control module. The PWM duty cycle variation will result in an analog signal (electrical tension), which is properly conditioned as a reference value to the PID controller.

5. THE AUTOTHROTTLE SYSTEM AND THE QUADRANT ASSEMBLY IMPLEMENTATION AND PERFORMANCE EVALUATION

Several hours of flight tests have shown that the designed autothrottle system has successfully achieved compliance with the IAS control aims. It is clear from Fig. 6 that the acceleration response produced by the digital PID controller follows the reference signals with minimum delay, which will consequently influence the IAS curve. Still from Fig. 6 it is noted that IAS adjustment has produced acceptable overshoot levels as well as excellent transitory responses. For this essay, overshoot level achieved 0,6%, which fully satisfies the initial IAS adjustment objectives with minimum overshoot value (Ogata, 2000). Stationary response reached values of 0,1%. Additional flight tests were run in order to re-check the above-mentioned results. They have reproduced the same levels of accuracy, which allows to consider the heuristic methods proposed here, so that an optimal and robust controller could be achieved.

The physical throttle quadrant has also presented very good results. Figure 7 shows the DC motor angular response $\theta(s)$ to impulse, step and ramp input signals respectively. That means that the DC motor full characterization process has successfully produced a reliable model for that device, so that its transfer function complies to the real model.

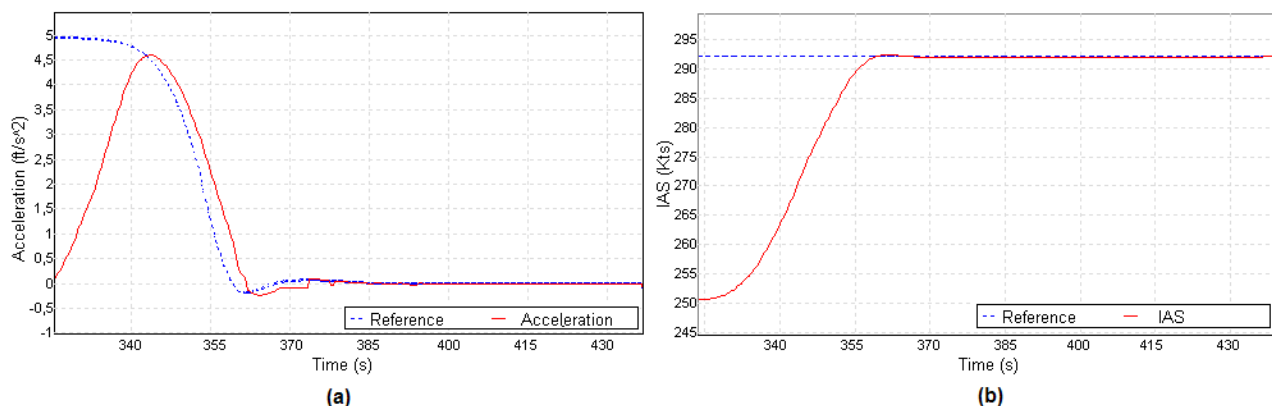


Figure 6. Aircraft acceleration (a) and indicated air speed (b) responses after the fine adjustment of the digital PID control through the insertion of β and N parameters. One may observe that the aircraft acceleration curve presents a quick response, reaching the reference signal more efficiently, which will generate a precisest IAS response as well.

The analog PID controller designed has also produced very satisfactory results. Figure 8 shows the controller response to a step input reference signal. It can be observed that it has achieved an error around 1.01%, which fully satisfies the initial control demands. Figure 9 brings the final plant response to a step input which, in practice, is the on-line reference signal incoming from the microcontroller. The plant includes the DC motor model, reduction gearbox gain, analog PID controller and sensing feedback linear potentiometer. As it can be noted the servo-system model response also fully satisfies the control demands, producing a very quick and precise angular throttle lever on-line reposition which, in practice, can be verified in flight essays, while SGVV calculates new aircraft acceleration levels.

The physical throttle quadrant is shown in the right side of Fig. 10. The left side of the figure shows the EMB-170 control panel whereas in the left bottom corner the virtual throttle quadrant is seen. While SGVV autothrottle module (through the digital PID controller) calculates new engine power levels by repositioning the virtual levers, the physical levers also have its angular position readjusted, so that the pilot can have the precise on-line visual level situation about the power requested to the aircraft's engines.

6. CONCLUSIONS

Simulation flight tests have shown very satisfactory results on the digital PID controller design, through the proposed methods. The insertion of the fine adjustment parameters on both proportional (β) and derivative (N) bands was extremely

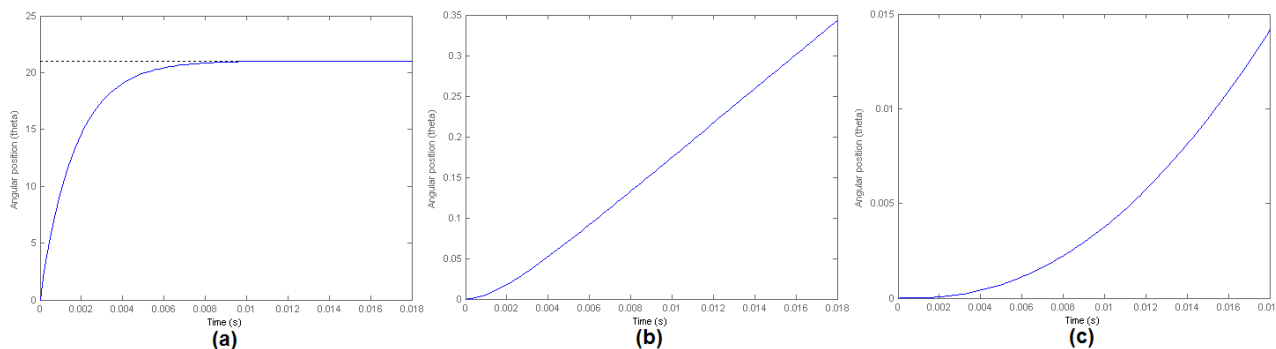


Figure 7. DC motor shaft angular position responses to impulse (a), step (b) and ramp (c) input reference signals respectively, coupled to the reduction gearbox. That means that the obtained DC motor transfer function represents the device dynamics with great precision.

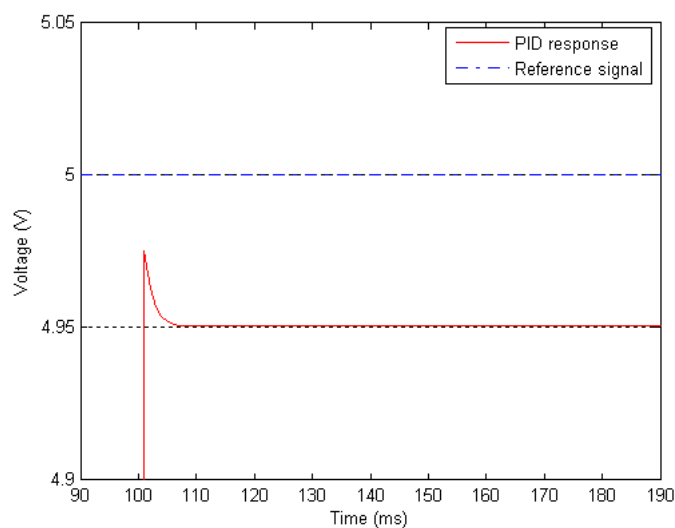


Figure 8. Analog PID controller response to a 5V step input signal, obtained from the SIMULINK model. It can be noted that control actions stabilize the output signal with 1.01% error.

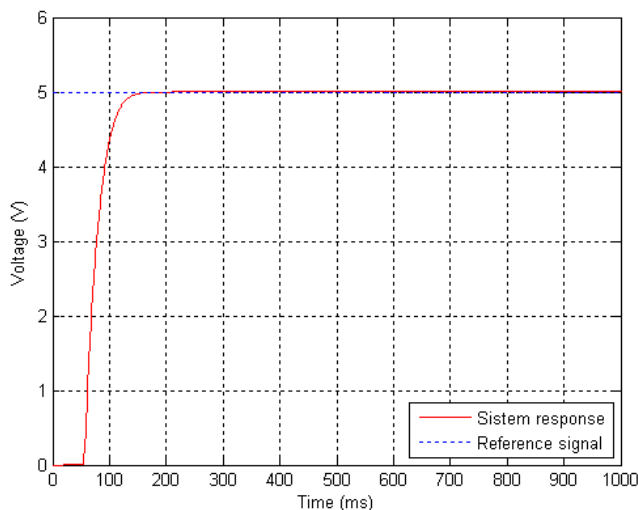


Figure 9. Final plant response to a 5V step input signal, which acts as the reference control signal incoming from the microcontroller. The designed servo-system has successfully achieved very good precision levels on the throttle levers angular reposition.

important to the controller efficiency achievement. Simulation plots confirmed that the methodology employed in this work results a more robust control systems for the inertial acceleration stabilization problem than to conventional classic design techniques. The digital autothrottle system presented very satisfactory results in all circumstances, even when in

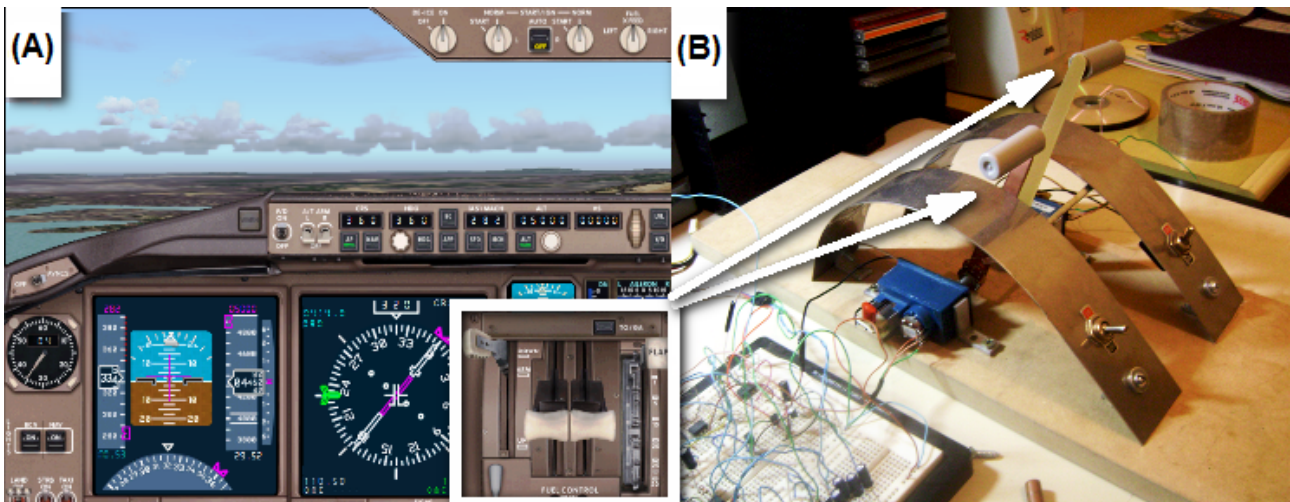


Figure 10. Autothrottle system prototype in running mode. Figure (A) shows the EMB-170 control panel, in cruise mode flight essay. Note the virtual throttle quadrant on the left bottom side of (A), inside the white square. From fig. (B), it can be seen the physical levers being readjusted on-line, accordingly to the virtual levers position.

the presence of high frequencies noise conditions, for instance, severe windshear conditions. The mechatronic throttle quadrant was successfully designed. Experimental techniques on full characterization of the DC motor proved to be efficient. The analog PID controller design process has also been successfully developed, since the initial aims were reached.

Future works includes the incorporation of an autonomous phase of flight change detection module, considering an intelligent self-reconfigurable adaptive controller, by using *Kalman* estimators, which will autonomously calculate the controller parameters for each flight situation.

7. ACKNOWLEDGEMENTS

The authors gratefully acknowledge the contribution of Engineer Thiago Cestari from Embraer for the crucial technical aid which refers to the validation of many results from the simulated aircraft, such as the aircraft envelopes and the autothrottle system as well.

8. REFERENCES

- Etkin, B.; Reid, L. D., 1996, *Dynamics of Flight, Stability and Control*, 3rd ed., JOHN WILEY SONS, INC., New York, USA.
- Ogata, K., 2000, *Engenharia de Controle Moderno*, 3rd ed., LTC, Rio de Janeiro, Brazil.
- Oliveira, Vilma A., 2005, *Sistemas de Controle: aulas de laboratorio*, 8th Ed., EESC/USP, Sao Carlos, Brazil.
- Pratt, R. W., 2005, *Flight Control Systems*, Volume 184, AIAA, Cambridge, UK.
- Rauw, Marc, 2001, FDC 1.2, *A Simulink Toolbox for Flight Dynamics and Control Analysis*, Second Edition, Delft University of Technology - Faculty of Aerospace Engineering Disciplinary Group for Stability and Control, Netherlands.
- Rolfe, J. M.; Staples, K. J., 1986, *Flight simulation*, Cambridge University Press, New York, USA.
- Roskan, Jan, 2001, *Airplane Flight Dynamics And Automatic Flight Controls*, Part I, DAR Corporation, Lawrence/Kansas, USA.
- Sampaio, R. C. B., 2008, *Avionic systems development based on flight simulator*, Proceedings of XVI SIICUSP, Ed. USP, São Paulo, Brazil.

9. Responsibility notice

The authors are the only responsible for the printed material included in this paper